JOURNAL OF Applied Polymer SCIENCE

Elucidation of Polymer Wear Resistance via Nanoscale Healing and Fracture of Sintered Polystyrene Particles

H. Mohammadi, N. Mohammadi, M. Kheirabadi
Department of Polymer Engineering and Color Technology, Loghman Fundamental Research Group, Amirkabir University of Technology, Tehran, Iran
Correspondence to: N. Mohammadi (E-mail: mohamadi@aut.ac.ir)

ABSTRACT: Polymer wear resistance evolution was studied based on nanoscale healing and fracture of a model polyinterface system: sintered film of uniform submicron polystyrene particles. The observed phenomenon was divided into three regimes namely interdiffusion, trough, and recovery, respectively. Film annealing up to 10 min in interdiffusion regime enhanced wear resistance with a 3.8 power dependence on interpenetration depth. Further annealing led to a severe wear resistance decrease, trough regime. Wear resistance then showed a sharp increase followed by a gradual rise to a plateau, recovery regime. Surfactants preservation during film formation shifted whole wear resistance-annealing time curve to shorter times, decreased differentiations among observed regimes and reduced wear resistance power dependence on interpenetration depth to 2.3. Aforementioned regimes were also discernible in impact strength-annealing time curves but without the steep rise of the recovery regime. Wear resistance scaled impact strength with a 0.67 power by omitting trough regimes data points. © 2012 Wiley Periodicals, Inc. J. Appl. Polym. Sci. 000: 000–000, 2012

KEYWORDS: annealing; fracture; impact resistance; interfaces; nanoparticles; nanowires; nanocrystals

Received 6 February 2012; accepted 18 August 2012; published online
DOI: 10.1002/app.38480

INTRODUCTION

Wear is a critical issue, which affects the successful performance of nanoscale viable devices with moving parts such as NEMS, nanoelectromechanical systems.[1] Polymer applications in such technical parts are considerable and grow rapidly.[2] Wear of polymers is mainly governed by their bulk physicochemical nature, involved surfaces and interfaces and microstructural properties immediately ahead of an advancing crack tip.[3,4] Therefore, extending applications of polymers with performances mainly affected by their wear characteristics needs basic knowledge on their structure–wear relationship.[5]

A new approach for investigating polymer microstructure/wear resistance correlation has been initiated by Mohammadi et al.[6] They used film formation process of high glass transition temperature, T_g, direct emulsified latex particles containing narrow molecular weight distribution polystyrene (PS) followed by grinding the film back to original particles or small clumps of them. The interpenetration depth of partially healed sintered PS particles was found as the key governing parameter of wear resistance build-up to a maximum.[6] However, further annealing led to a shallow depth wear resistance decrease.[6] The used model system may mask some of the possible complexities of real polymer systems such as different free volume distributions, broad molecular weight distributions, and distinct chain end loci, which could affect their fracture properties. Milner et al.[7] theoretically proved the free volume probability distribution shift to lower sizes by polymer densification through processing or polymerization. The fracture of nanovoids containing polymers,[8,9] experiences a brittle to ductile transition by the ligament thickness decrease beyond a finite threshold and vice versa. Such a threshold ligament thickness was estimated to be about 18 nm for PS.[10] On the other hand, Aradian et al.[11] realized several temporal regimes during the evolution of asymmetric polymer junctions, even between chemically identical melts with different molecular weights. This phenomenon leads to interfacial layering during the processing of polymers with broad molecular weight distributions.[12] Janarthanan et al.[13] ascribed higher fracture energy of polymeric joints than what was expected to the periodic tortuous crack growth path between the interface and low entanglement density component. Finally, various strength-interpenetration depth scaling powers reported for the interfacial healing of polymers was attributed to the chain ends initial loci.[14–16] While chain ends uniform distribution through the bulk favors second power, chain ends localization at the interface biases first power.

Table I. The Recipe of Styrene Emulsion Polymerization

Ingredients	Weight (g)
Styrene	14
Water	56
KPS	0.07
SLS	0.027
Triton X-100	0.42
KOH	0.011
CCl_4	0.14

Scrutinizing the interfacial healing problem for real polymeric systems requires application of emulsion polymerized latex particles. Broad molecular weight distribution and peculiar free volume distribution were reported for emulsion polymerized latex particles with special molecular characteristics and sizes. Polymer molecular weight, chain ends nature, and particle size were reported as the most important parameters dictating the nanostructure of colloidal particles.[17,18] Two hundred nanometer emulsion polymerized PS particles with molecular weight of about 10^6 g/mol showed chain ends localization at the water interface and reverse core-shell morphology.[17] In other words, during the course of polymerization, entering monomer to the growing particles, diffuses to their central parts, while the dead polymer chains localize at water interface adopting collapsed conformation.

In this research work, polymer wear resistance was further elucidated based on the nanoscale healing and fracture of sintered emulsion polymerized uniform PS particles with and without surfactants. The concept of formation and evolution of two nanoscopic phases with different entanglement densities at particles interface and core was used to rationalize the observed anomalies. A new model is also proposed for correlating polymer wear resistance to interpenetration depth at short annealing times. The wear resistance-impact strength relationship was scrutinized and rationalized. Extrapolating the efforts on a polyinterface system to an interface-free one, bulk, would eventually contribute to elucidation of polymer wear micro-mechanisms.

EXPERIMENTAL

Materials

Styrene was purchased from Merck and its inhibitor was removed by its passage through an alumina packed column. Mixed surfactant system of sodium lauryl sulfate (anionic, Fisher scientific) and Triton X-100 (nonionic, Rohm & Haas) was used. Potassium persulfate (KPS), potassium hydroxide (KOH) and carbon tetrachloride (CCl_4) were also received from Merck and used as initiator, pH regulator, and chain transfer agent, respectively. Double-distilled water was supplied by Kimidaroo and used as the polymerization media.

Emulsion Polymerization

Uniform PS particles were synthesized by emulsion polymerization. The ingredients of the recipe, Table I, were added to 120 ml glass bottles, sealed and set in a tumbling reactor and turned over and over at 60 rpm and 60°C for 24 h.

Polymer and Particle Characterizations

Polymer molecular weight and molecular weight distribution were analyzed by gel permeation chromatography (GPC, 150C, WATERS). Dried latex average particle size and size distribution were determined using size analyzing program, ImageJ 1.45, on the transmission electron microscopy (TEM, Philips 300) photomicrograph and confirmed by photon correlation spectroscopy (Coulter Counter N4MD) on the latex.

Particles Cleaning and Sintering

After drying the latex at 40°C for one week, nonionic and ionic surfactants were removed by repeated extraction with methanol and hot distilled water, respectively. The final wet powder was dried at 60°C for 24 h. The cleaned and dried PS particles were then sintered to void free, fully dense films using a hot press at 100°C for 40 min under a pressure of 9 MPa. These conditions were just sufficient to minimize chains interdiffusion among the neighboring particles.[6] Parts of the synthesized and dried particles were sintered without removing their surfactants using the aforementioned conditions.

Film Annealing

The sintered films, 1 mm in thickness and 3.75 cm in diameter, were annealed at 140°C. To prevent sample distortion during the annealing process, it was placed within a steel O-ring spacer with same thickness and inner diameter and fixed between two smooth steel plates. Annealing was performed in a forced convection oven and 30 min were allowed for temperature equilibration. The fixture containing sample was taken out of the oven after prescribed annealing time and immediately quenched in 15°C tap water to inhibit further interdiffusion.

Impact Strength Measurement

Impact strength of each film was measured by falling weight technique at room temperature. The film was fixed between two glass plates with concentric circular holes to allow its impact by the spherical falling weight. The reported impact strength was extracted by dividing the applied energy, mgh, (0.13 J) to the multiple cracks length m, g, and h are falling weight mass (38.5 g), earth acceleration gravity, and initial height of the falling weight (35 cm), respectively. The procedure was repeated on at least three replicates and average impact strength values were reported.

Wear Resistance Measurement

A disc on drum type abrader (Monsanto) was used for the wear test. Polymer disc, 1 mm in thickness and 1 cm in diameter, was adhered to a 15 mm thick Bakelite® disc and clamped inside the sample holder. It was then worn in a pure sliding motion against a grade 220 aluminum oxide sand paper (RMX022, Germany), covering a rotating cylinder (radius of 150 mm and length of 500 mm) with linear speed of 21 m/min. The specimen holder arm moves parallel to the cylinder axis and is located by 1500 g mass, providing a contact normal force of 15 N. Average weight loss per 5.25 m of sliding distance for at least three replicates was reported.

RESULTS

Figure 1 shows the TEM photomicrograph of the emulsion polymerized PS particles. Average particle size and size

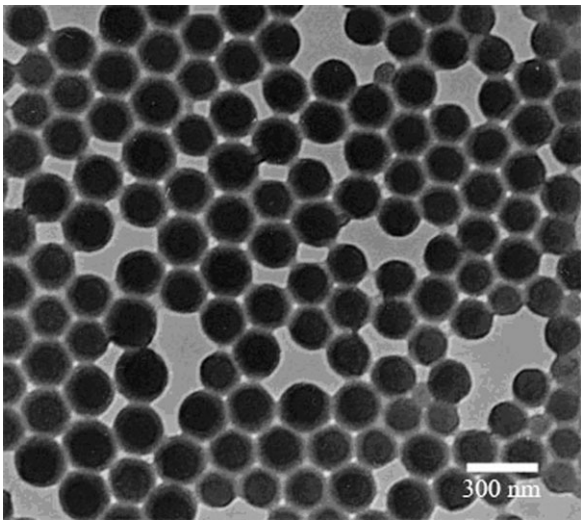

Figure 1. Transmission electron photomicrograph of uniform polystyrene particles.

distribution were 200 nm and 1.07, respectively. Particle size distribution was estimated by the volume average to the weight average particle size ratio. Photon correlation spectroscopy on the latex system confirmed the extracted particle size and size distribution. Weight average molecular weight and molecular weight distribution of the synthesized PS were 10^6 g/mol and 3.7, respectively. The molecular weight trace is simply a broad single peak one.

Double logarithmic plots of wear resistance versus annealing time for surfactants free and surfactants containing PS films are illustrated in Figure 2. Three regimes: interdiffusion, trough, and recovery could be assigned to the wear resistance evolution data. In both curves, surfactants free and surfactants containing PS films, wear resistance increased to a maximum in short annealing times (interdiffusion regime), declined abruptly

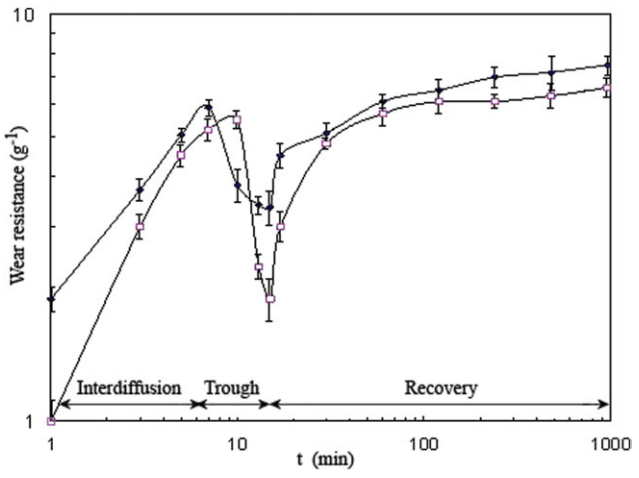

Figure 2. Double logarithmic plots of wear resistance versus annealing time for surfactant free ([○]) and surfactants containing ([▲]) PS films. The lines through data points were drawn to guide the eye. [Color figure can be viewed in the online issue, which is available at wileyonlinelibrary.com.]

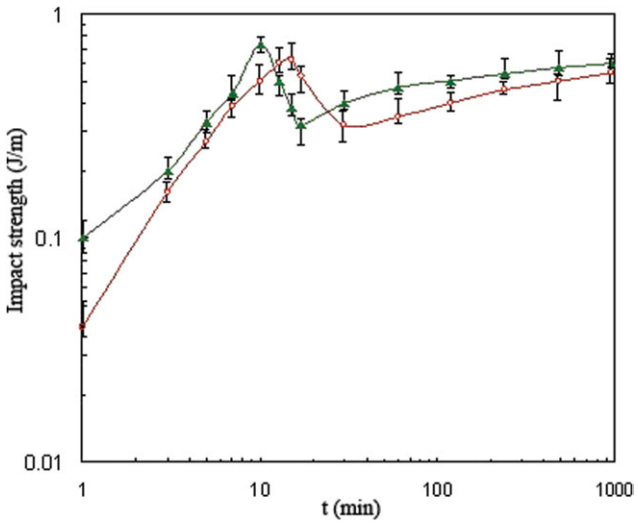

Figure 3. Double logarithmic plots of impact strength versus annealing time for surfactant free ([○]) and surfactants containing ([▲]) PS films. The lines through data points were drawn to guide the eye. [Color figure can be viewed in the online issue, which is available at wileyonlinelibrary.com.]

(trough regime) and recovered again (recovery regime). Nevertheless, the wear resistance evolution curve of surfactants containing PS films shifted to shorter annealing times with reduced differentiations among various regimes.

Three regimes of nanostructural evolution regarding surfactants free and surfactants containing PS films were also discernible in impact strength versus annealing time curves but with a major difference in their recovery regimes, Figure 3. Both curves showed gradual rise in the recovery regimes in contrast to the wear resistance-annealing time plots with an initial steep increase followed by a slow rise, Figure 2. Impact strength-annealing time curve of surfactants containing samples also shifted to shorter annealing times with roughly the same drop amplitude at trough regime as surfactants free samples.

Double logarithmic plot of wear resistance versus impact strength for all studied samples is shown in Figure 4. By excluding the trough regimes data points, a power law correlation with a 0.67 exponent was found.

DISCUSSION

Wear resistance versus annealing time curve for surfactants free PS films along with their representative nanostructural depicting cartoons is shown in Figure 5. After sintering the particles at polymer T_g, they deform to dodecahedron close pack forms indicated schematically in Figure 5.[19] Film annealing at 140°C activates chain interdiffusion at interfaces and results in wear resistance build-up. In the interdiffusion regime, chains cross the interface of neighboring particles and form new entanglements. Accordingly, interpenetration depth determines crack growth molecular mechanisms and paths, chain rupture, and/or pull out for the former and through particles interface and/or bulk for the latter.[6] However, interdiffusion process may be complicated due to particles inverted core-shell morphology formed

Applied Polymer SCIENCE

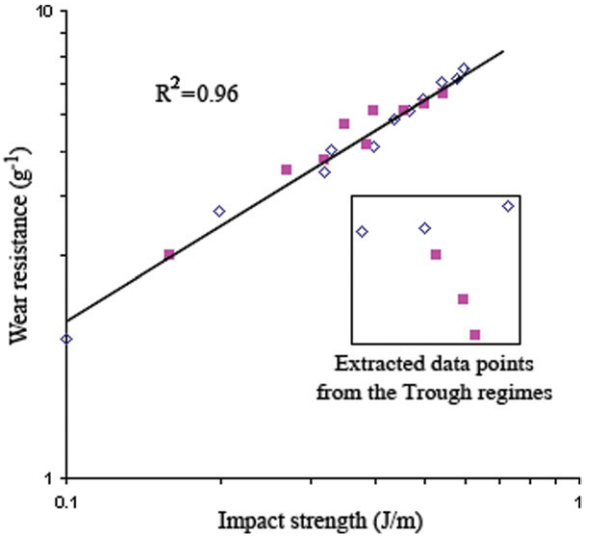

Figure 4. Double logarithmic plot of wear resistance versus impact strength for all studied samples: surfactant free ([◇]) and surfactants containing ([■]). [Color figure can be viewed in the online issue, which is available at wileyonlinelibrary.com.]

during emulsion polymerization. Here, each particle is composed of a shell containing high entanglement density chains with end localized at water interface along with low entanglement density cores.[17] Chains collapsed conformation at the interface of sintered PS particles enhances their short time interdiffusion rate. de Gennes introduced the chain explosion diffusion concept to describe very high diffusion coefficient under the contribution of chain entropic relaxation.[20] The enhanced diffusion coefficient, apparent, is designated by D^* and estimated to be equal to:[6]

$$DD^{*-1} = \left(t\tau^{-1}\right)^{0.5} \tag{1}$$

where t and τ are the annealing time and chain relaxation time, respectively. Reptative diffusion coefficient of unperturbed polymer chain; however, scales weight average molecular weight, M_w, as follow:

$$D \propto M_w^{-2} \tag{2}$$

Using reptative diffusion coefficient of 20.4×10^{-16} cm^2 s^{-1} for PS with molecular weight of 1.5×10^5 g mol^{-1} at 140°C,[21] the diffusion coefficient of the studied PS with molecular weight of 10^6 g mol^{-1} was estimated 4.7×10^{-18} cm^2 s^{-1}. On the other hand, the relaxation time of the emulsion polymerized PS at 140°C was calculated 1615 min using eq. (3) and the relaxation time of PS with molecular weight of 4.2×10^5 g mol^{-1}.[6]

$$\tau \propto M_w^3 \tag{3}$$

Inserting D and τ in eq. (1), D^* was calculated and plotted versus annealing time, Figure 6. Corresponding interpenetration depths, l, were also determined using eq. (4) and plotted versus annealing time in Figure 6.

$$\ell^2\pi = 16D^*t \tag{4}$$

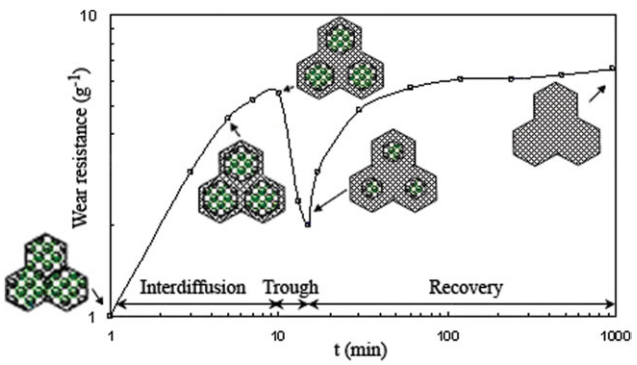

Figure 5. Double logarithmic plot of wear resistance versus annealing time for surfactant free PS films with their representative nanostructural depicting cartoons. The line through data points was drawn to guide the eye. [Color figure can be viewed in the online issue, which is available at wileyonlinelibrary.com.]

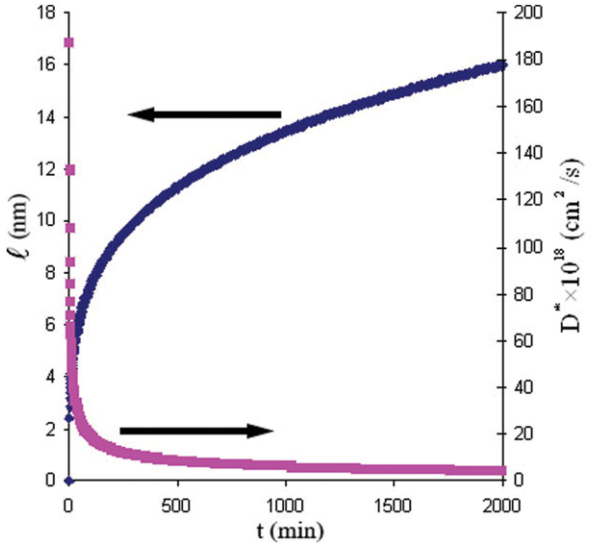

Figure 6. Apparent diffusion coefficient and interpenetration depth versus annealing time for surfactant free sintered PS films. [Color figure can be viewed in the online issue, which is available at wileyonlinelibrary.com.]

By the onset of annealing, the calculated apparent diffusion coefficient decreased sharply and reaches 10% of its initial magnitude after 5 min. Meanwhile, the interpenetration depth grows to 3.5 nm leading to a 7 nm thick ligament among the cores of the adjacent particles, Figure 5. Chain interdiffusion at particles interface forms two phases with nanostructural disparity namely reach and lean in entanglement density at the interface and bulk of the particles, respectively, Figure 5. Beyond 5 min of annealing, the crack growth path may change alternatively between the interface and the bulk of particles.[13] Consequently, wear resistance increases to a maximum but with a lower slope, Figure 5.

Double logarithmic plot of surfactants free samples wear resistance versus their interpenetration depth in the interdiffusion

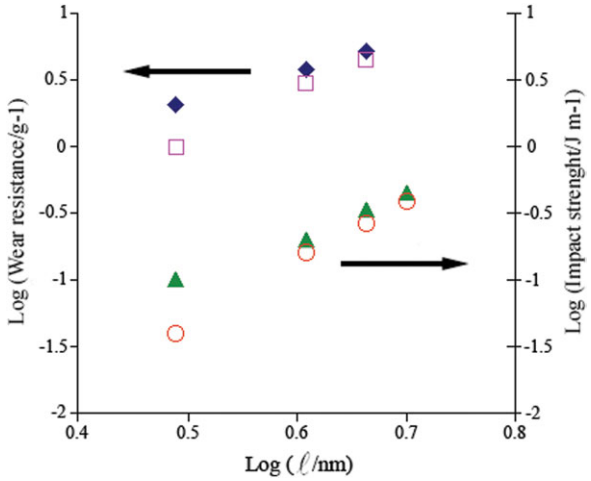

Figure 7. Double logarithmic plots of wear resistance and impact strength versus interpenetration depth of surfactant free ([□] wear, [○] impact strength) and surfactants containing ([◆] wear, [▲] impact strength) PS films in interdiffusion regime. [Color figure can be viewed in the online issue, which is available at wileyonlinelibrary.com.]

regime shows a 3.8 power dependence, Figure 7. Surfactants preservation during film formation reduces wear resistance power dependence on interpenetration depth to 2.3, Figure 7. As PS diffusion coefficient does not change with surfactants preservation below its relaxation time,[21] similar interpenetration depths at comparable annealing times was considered for surfactants containing samples. In other words, annealed surfactants free and surfactants containing samples acquired similar interpenetration depth at the same annealing times.

Elastic energy release rate dependence on the square power of applied stress[22] led to second and fourth power correlations between interfacial fracture energy and interpenetration depth based on Wool[14] and de Gennes–Tirrell[15,16] interfacial healing models, respectively. While Wool[14] assumed uniform chain ends distribution through the bulk, de Gennes and Tirrell groups[15,16] considered chain ends localization at the interface. Combining linear dependence of wear energy on interfacial fracture energy for systems with crack growth through the interface,[3] wear resistance proportionality to wear energy[23,24] and basic interfacial healing models, following scaling equations were deduced:

$$\text{Wear resistance} \propto l^2 \text{ (based on Wool's Model)} \quad (5)$$

$$\text{Wear resistance} \propto l^2 \text{ (based on de Gennes/Tirrell's Model)} \quad (6)$$

Models were well fitted on the experimentally found wear resistance dependences on interpenetration depth: de Gennes–Tirrell's for surfactant free and Wool's for surfactants containing samples, Figure 7. Surfactants preservation facilitates interfacial chain ends redistribution through the bulk during particles sintering and initial film temperature equilibration at annealing stage via lowering the polymer T_g. Therefore, the power dependence of wear resistance on interpenetration depth changed from 3.8 to 2.3, Figure 7. A third power dependence of wear resistance on interpenetration depth was previously reported for partially annealed films of sintered PS particles in their interdiffusion regime.[6] Uniform PS particles with comparable size but lower molecular weight and narrow molecular weight distribution were used. The artificial particles prepared through direct emulsification technique led to chain ends distribution through the bulk. Higher power dependence than the model prediction for that system, may be attributed to the nature of chain ends[18] and residual solvent behind the particle preparation step.

By further annealing left beyond during the observed maximum, Figure 5, wear resistance declined abruptly into the trough regime. The nanostructural evolution of sintered PS films through interdiffusion increased particles interfacial thickness while reduced their core size resulted in shifting their free volume probability distribution to lower sizes.[7] Crossing the interfacial threshold ligament distance, 9 nm, by the high entanglement density phase resulted in wear resistance abrupt drop because of a tough-brittle transition. It is worth mentioning that in the model systems with narrow molecular weight distribution chains engulfed in uniform submicron particles, the through regime is omitted or has a shallow depth.[6] However, theoretical critical ligament distance was estimated 18 nm for nanovoids containing PS.[10] The toughened PS with poly(styrene-block-butadiene) chains increased the inter-ligament distance for a brittle-tough transition to about 50 nm.[25] Broad molecular weight distribution of the studied polymer, the collapsed nature of interfacial chains and the nanostructural complexity of the latex particles core may be nominated as possible reasons for the observed lower threshold ligament thickness.

The tough-brittle transition was reversed by further annealing but in a two step process, Figure 5 (recovery regime). In other words, the wear resistance corresponding the trough minimum is instantaneously recovered with a steep build-up followed by a gradual increase toward a plateau. The observed discontinuity in wear resistance build-up after crossing the trough minimum was ascribed to instantaneous void mixing between high entanglement density and low entanglement density regions to relief their osmotic pressure disparity. Huge osmotic pressure difference in film formation of emulsion polymerized latex particles with complex internal structure differentiates them from artificially made particles with mild recovery regime. Film nanostructure will then continue gradual change toward virgin PS with less than 10 vol % of hole free.[7] Osmotic pressure driven transition was not detected in impact strength evolution curves, Figure 3, probably due to the test insensitivity. Impact strength is recalled as a bulk material characteristic, while wear resistance is mainly governed by the localized stress amplitude ahead of growing crack tip.[3] Since, the stability of craze fibrils is controlled by their fracture resistance, polymer wear is well correlated with the stress intensity factor rather than impact strength, a bulk property.[3] Therefore, combination of wear resistance and impact strength results can differentiate various involved fracture micro-mechanisms with bulk and/or localized characteristics. Detection of nanostructural evolution in interdiffusion and trough regimes with impact strength test was attributed to crack growth path selectivity through the interfaces diminishing at longer annealing times.

The power dependence of impact strength on interpenetration depth for surfactants free and surfactants containing samples

were 4.7 and 3, respectively, Figure 7. A higher exponent for impact strength dependence on interpenetration depth in comparison with wear resistance was expected due to the test bulk character, energy driven phenomenon.[3] An amplification factor of 1.5 was found experimentally for estimating impact strength power dependences on interpenetration depth from wear resistance-impact strength correlation for the studied samples, Figure 4. A linear dependence for the wear resistance of several polymers on their tensile facture energy, also a bulk property was reported[26] and is known as Ratner–Landcaster correlation. In the interfacial healing of samples with chain ends distribution through the bulk or surfactants preserved sintered nanoparticles, second and third exponents for wear resistance and impact strength dependences on interpenetration depth was expected, respectively. Chain ends localization at the interface; however, changes the exponent of wear resistance and impact strength dependences on interpenetration depth to four and six. Lower exponent of the impact strength dependence on interpenetration depth, 4.7, for surfactants free samples was attributed to interfacial layering[7] due to broad molecular weight distribution and possible contribution of chain ends nature.[18]

CONCLUSIONS

Wear resistance-interpenetration depth correlation was modeled for interdiffusion regime of PS polyinterface systems, which led to four and two power dependences with chain ends localization at the interface and uniform distribution through the bulk, respectively. Experimentally determined exponent for wear resistance dependence on interpenetration depth for surfactant free sintered PS films with chain ends localization at the interface, 3.8, declined to 2.3 by surfactants preservation. Apparently, surfactants preservation facilitates chain ends redistribution from the interface to through the bulk during the initial annealing period. A 0.67 power dependence was found for wear resistance correlation with impact strength provided that the data points of trough regimes originated from the complexities of the studied system was excluded. Third and sixth powers were estimated for impact strength dependence on interpenetration depth for interfaces crossed by chain ends coming through the bulk or localized at the interface, respectively. While experimental confirmation was found for the system with chain ends diffusion through the bulk, much lower exponent, 4.7, was detected for the system with chain ends localization at the interface.

REFERENCES

1. Gotsmann, B.; Duerig, U. T.; Sills, S.; Formmer, J.; Hawker, C. *J. Nano Lett.* **2006**, *6*, 296.
2. Xu, D.; Karger-Kocsis, J.; Schlarb, A. K. *eExpress Polym. Lett.* **2009**, *3*, 126.
3. Omar, M. K.; Atkins, A. G.; Landcaster, J. K. *J. Phys. D: Appl. Phys.* **1986**, *19*, 177.
4. Tervoort, T. A.; Visjager, J.; Smith, P. *Macromolecules* **2002**, *35*, 8467.
5. Lucas, A. de A.; Ambrosio, J. D.; Otaguro, H.; Costa, L. C.; Agnelli, J. A. M. *Wear* **2011**, *270*, 576.
6. Mohammadi, N.; Klein, A.; Sperling, L. H. *Macromolecules* **1993**, *26*, 1019.
7. Milner, S. T.; Lacasse, M. D.; Graessely, W. W. *Macromolecules* **2009**, *42*, 876.
8. Yampolskii, Y. *Macromolecules* **2010**, *43*, 10185.
9. Dutriez, C.; Satoh, K.; Kamigaito, M.; Yokoyama, H. *Macromolecules* **2007**, *40*, 7433.
10. van Melick, H. G. H.; Govaert, L. E.; Meijer, H. E. H. *Polymer* **2003**, *44*, 457.
11. Aradian, A.; Saulnier, F.; Raphael, E.; de Gennes, P. G. *Macromolecules* **2004**, *37*, 4664.
12. Chang, C. J.; Lee, Y. H.; Chiang, C. J.; Lee, Y. P.; Chien, H. C.; Shih, W. P.; Cheng, Y. Y.; Dai, C. A.; Chang, C. H. *J. Polym. Sci. B: Polym. Phys.* **2010**, *48*, 1834.
13. Janarthanan, V.; Stein, R. S.; Garrett, P. D. *Macromolecules* **1994**, *27*, 4855.
14. Wool, R. P. Polymer Interfaces: Structure and Strength; Hanser/Gardner: New York, **1995**.
15. de Gennes, P. G.; Seances, C. R. *Acad. Sci. Ser. B* **1980**, *291*, 219.
16. Prager, S.; Tirrell, M. *J. Chem. Phys.* **1981**, *75*, 5194.
17. Yang, S. I.; Klein, A.; Sperling, L. H.; Casassa, E. F. *Macromolecules* **1990**, *23*, 4582.
18. Kim, S. D.; Klein, A.; Sperling, L. H.; Boczar, E. M.; Bauer, B. *J. Macromolecules* **2000**, *33*, 8334.
19. Nawaz, Q.; Rharbi, Y. *Langmuir* **2010**, *26*, 1226.
20. de Gennes, P.G. *C. R. Acad. Sci. Ser. IIb: Mec. Phys. Chim. Astron.* **1995**, *321*, 363.
21. Kim, K. D.; Sperling, L. H.; Klein, A.; Hammouda, B. *Macromolecules* **1994**, *27*, 6841.
22. Griffith, A. A. *Philos. Trans. R. Soc. London Ser.* **1920**, *A221*, 163.
23. Colaco, R.; Gispert, M. P.; Serro, A. P.; Saramago, B. *Tribol. Lett.* **2007**, *26*, 119.
24. Geringer, J.; Forest, B.; Combrade, P. *Polym. Eng. Sci.* **2007**, *47*, 633.
25. Lach, R.; Weidisch, R.; Janke, A.; Knoll, K. *Macromol. Rapid Commun.* **2004**, *25*, 2019.
26. Lancaster, J. K. *Tribol. Conv.* **1969**, *7*, 100.